ACS OMEGA

Open Access

http://pubs.acs.org/journal/acsodf

Article

Detection of α-Thrombin with Platelet Glycoprotein Ibα (GP1bα) for the Development of a Coagulation Marker

Doogie Oh, Yun Jin Chae, Jie Ying Teoh, Bora Yim, Dongwon Yoo, Yongdoo Park,* and Jongseong Kim*

Cite This: *ACS Omega* 2024, 9, 13418−13426

Read Online

ACCESS | Metrics & More | Article Recommendations | Supporting Information

ABSTRACT: The detection of prothrombotic markers is crucial for understanding thromboembolism and assessing the effectiveness of anticoagulant drugs. α-Thrombin is a marker that plays a critical role in the coagulation cascade process. However, the detection of this enzymatic molecule was hindered by the absence of an efficient modality in the clinical environment. Previously, we reported that one α-thrombin interacts with two α-chains of glycoprotein Ib (GPIbα), i.e., multivalent protein binding (MPB), using bioresponsive hydrogel nanoparticles (nanogels) and optical microscopy. In this study, we demonstrated that GPIbα-mediated platforms led to the highly sensitive and quantitative detection of α-thrombin in various diagnostic systems. Initially, a bioresponsive nanogel-based surface plasmon resonance (nSPR) assay was developed that responds to the MPB of α-thrombin to GPIbα. The use of GPIbα for the detection of α-thrombin was further validated using the enzyme-linked immunosorbent assay, which is a gold-standard protein detection technique. Additionally, GPIbα-functionalized latex beads were developed to perform latex agglutination (LA) assays, which are widely used with hospital diagnostic instruments. Notably, the nSPR and LA assays exhibited a nearly 1000-fold improvement in sensitivity for α-thrombin detection compared to our previous optical microscopy method. The superiority of our GPIbα-mediated platforms lies in their stability for α-thrombin detection through protein−protein interactions. By contrast, assays relying on α-thrombin enzymatic activity using substrates face the challenge of a rapid decrease in postsample collection. These results suggested that the MPB of α-thrombin to GPIbα is an ideal mode for clinical α-thrombin detection, particularly in outpatient settings.

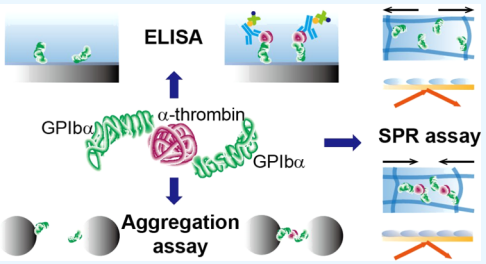

1. INTRODUCTION

Measurement of α-thrombin in clinical practice is highly beneficial for the treatment of thrombosis and embolism initiated by blood clot formation. α-Thrombin is produced by the proteolytic cleavage of prothrombin, which is initiated during the clotting process. This serine protease plays an important role in blood coagulation by converting fibrinogen to fibrin monomers and activating factor XIII for polymerization, resulting in the trapping of red blood cells and platelets.[1] Such characteristics of α-thrombin in the clotting cascade render this enzyme a candidate marker for hypercoagulability.[2] Currently, the D-dimer test is used as a diagnostic standard for determining blood clotting disorders;[3] however, it is mainly recommended to exclude the possibility of thrombotic diseases with a negative result. Prothrombin time with an international normalized ratio (PT/INR) and activated partial thromboplastin time (aPTT) are also measured to assess the risk of stroke, systemic embolism, and bleeding.[4−8] However, both methods are unsuitable for accurate and timely prediction of thrombotic disorders because they measure the resulting coagulation time rather than molecular markers. Therefore, rapid and sensitive detection of α-thrombin in patients is urgently needed.

Application of new modalities like as electronic modulation is typically adopted in materials science,[9] and meanwhile, employment of new binding modes in sensing methods can revolutionize clinical practices. For decades, the potential function of α-thrombin involving the α-chain of glycoprotein Ib (GPIbα) has been investigated. At sites of vascular injury, the binding of platelet glycoprotein Ibα (GPIbα) to the von Willebrand factor (vWF) A1 domain leads to positive feedback-driven recruitment of circulating platelets, thereby initiating hemostatic plug formation.[10−15] α-Thrombin has been revealed to have two distinct binding sites to GPIbα with high (exosite II) and moderate (exosite I) affinities, as demonstrated by various methods, including isotope-labeled competition assays, X-ray crystallography, surface plasmon resonance (SPR) analysis, etc.[16−19] Although the functional importance of their binding in the context of clot formation is

Received: January 1, 2024
Revised: February 5, 2024
Accepted: February 21, 2024
Published: March 5, 2024

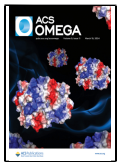

controversial,[1,20−25] GPIbα dimerization via α-thrombin was confirmed by X-ray crystallography and biochemical assays.[17,26]

Previously, we demonstrated an optical imaging method that allowed direct observation of GPIbα dimerization induced by α-thrombin binding.[26] This method, which relies on receptor-functionalized nanogels, contributed to our understanding of receptor multimerization and can be used for the detection of ligands via specific multivalent protein binding (MPB). However, microscopic imaging lacks sensitivity for the accurate quantification of target molecules and requires sophisticated instrumentation. To overcome these limitations, bioresponsive nanogels have been employed as sensing platforms in surface plasmon resonance (SPR) analysis to investigate the MPB of programmed cell death protein 1, interleukin-2 (IL-2) receptor α, and the receptor-binding domain of severe acute respiratory syndrome coronavirus 2 (SARS-CoV-2) to their ligands.[27−30]

Herein, we developed biochemical assays using an MPB modality for the demonstration of α-thrombin detection, aiming for the early diagnosis of thromboembolism and preemptive treatments of those patients. Upon α-thrombin binding, the GPIbα-functionalized platform forms a cross-linked network, thereby leading to changes in properties such as refractive index (RI). First, SPR analysis was conducted to measure the α-thrombin concentration using the nanogel as the sensing platform. A standard or a preincubation protocol was performed to determine the optimal experimental configurations for SPR signal intensification. For comparison, an enzyme-linked immunosorbent assay (ELISA) was also performed. To demonstrate whether MPB-sensing platforms are useful for the detection of α-thrombin in an outpatient setting, GPIbα-functionalized latex beads were tested for latex agglutination (LA) assays using dynamic light scattering (DLS) analysis and ultraviolet−visible (UV−vis) spectroscopy.

2. EXPERIMENTAL SECTION

2.1. Materials. All chemicals were used as received unless otherwise mentioned. *N*-Isopropylacrylamide (NIPAm), acrylic acid (AAc), *N*,*N*′-methylenebis(acrylamide) (BIS), ammonium persulfate (APS), poly(oxyethylene) sorbitan monooleate (Tween 80), *N*-hydroxysuccinimide (NHS), 1-ethyl-3-(3-(dimethylamino)propyl) carbodiimide (EDC), cysteamine, *Nα*,*Nα*-bis(carboxymethyl)-L-lysine hydrate (NTA), and nickel(II) chloride were purchased from Sigma-Aldrich (St. Louis, MO). Phosphate-buffered saline (PBS) was purchased from Welgene (Gyeongsan, Korea). 2-(*N*-Morpholino)ethanesulfonic acid (MES) was obtained from Biosolution (Seoul, Korea). 6-His-tagged GPIbα was purchased from Abnova (Taipei City, Taiwan). α-Thrombin was purchased from Haematologic Technologies, Inc. (Essex Junction, VT).

2.2. Synthesis of Hydrogel Nanoparticles (Nanogels). Hydrogel nanoparticles with a molar composition of 88% NIPAm, 10% AAc, and 2% BIS were synthesized via aqueous free-radical precipitation polymerization. NIPAm and BIS were dissolved in deionized water, followed by the addition of Tween 80. The mixture solution was then heated to 70 °C and purged with nitrogen gas. After 1 h, AAc was added to the mixture, which was then maintained under nitrogen for 10 min. To initiate the reaction, 1 mL of a 2 mM APS solution was added to the mixture. The reaction was performed for 6 h at 70 °C under nitrogen purging. The polymerized nanogel was purified by dialysis (Spectra-Por Dialysis Tubing, MWCO 50 kDa; Spectrum Laboratories, Inc., Piscataway, NJ) against deionized water for 3 days. Chemical and morphological characterizations of the nanogel were performed by ^{1}H nuclear magnetic resonance (NMR) spectroscopy (Figure S1) and atomic force microscopy (AFM) (Figure S2), respectively.

2.3. Nuclear Magnetic Resonance (NMR) Spectroscopy. ^{1}H NMR spectra were recorded using a Bruker Avance III 400 MHz spectrometer (Bruker, Karlsruhe, Germany). Data analysis was performed with the TopSpin 3.5 Software. NMR samples were prepared by dissolving 5 mg of NHs in 500 μL of DMSO-d_6.

2.4. Atomic Force Microscopy (AFM). The surface morphology of the microgel-modified SPR sensor chip was characterized by atomic force microscopy (AFM) (Park Systems, NX-10) in air. The images were acquired in a 2.5 × 2.5 μm^2 area at a scan rate of 0.5 Hz with 256 scan points and lines in the noncontact mode.

2.5. SPR Analysis. The lyophilized nanogel was diluted 100 times with MES buffer (pH 5.5, 0.1 M) for 30 min. Subsequently, 60 μL of the diluted nanogel solution was mixed with 10 μL of EDC (20 μg/μL in MES buffer) and 10 μL of NHS (40 μg/μL in MES buffer) and incubated for 5 min. A total of 20 μL of the GPIbα solution was added to the mixture to obtain a protein concentration of 1 μM, followed by incubation for 40 min. The mixture was centrifuged at 8000 rpm for 5 min. The supernatant was removed, and the concentrate was mixed with 100 μL of PBS. The centrifugation and mixing steps were repeated three times. The functionalized nanogels were stored at 4 °C.

To prepare the measurement and reference channels, gold sensor chips were cleaned with distilled water and treated with a 40 mM cysteamine aqueous solution for 30 min, followed by vacuum suction until completely dried. The activated sensor chip was loaded onto an imSPR system (iCluebio, Seongnam-si, Korea). The measurement and reference channels were injected with the corresponding nanogel solution (MES buffer) at a flow rate of 30 μL/min for 3 min. The unreacted nanogels were washed out by running the PBS buffer for 5 min. For SPR measurement, α-thrombin was diluted in PBS buffer at various concentrations and injected into the channels at a flow rate of 30 μL/min for 90 s, and the dissociation time was 120 s. The sensorgram was recorded by using the embedded imSPR-min software.

2.6. Ni-NTA-Mediated SPR Analysis. Lyophilized nanogels were diluted 100 times with MES buffer (pH 5.5, 0.1 M). Subsequently, 60 μL of the diluted nanogel solution was mixed with 10 μL of EDC (20 μg/μL in MES buffer) and 10 μL of NHS (40 μg/μL in MES buffer) and incubated for 5 min. A total of 20 μL of the NTA solution was added to the mixture to obtain a concentration of 5 mM NTA, followed by incubation for 40 min. The unreacted EDC, NHS, and NTA were removed by repeated centrifugation and resuspended in a PBS buffer. A $NiCl_2$ solution was added to obtain a final concentration of 0.5 mM and to form Ni-NTA nanogels. The functionalized nanogels were stored at 4 °C.

As in the previous SPR analysis, measurement and reference channels were created in the SPR instrument. These channels were injected with the Ni-NTA nanogel solution and washed with PBS to remove the unreacted nanogels. For SPR measurements, α-thrombin was diluted in PBS buffer at various concentrations and mixed with the GPIbα solution for preincubation. Subsequently, the mixture was injected into the channels at a flow rate of 30 μL/min for 90 s, and the

https://doi.org/10.1021/acsomega.4c00010
ACS Omega 2024, 9, 13418−13426

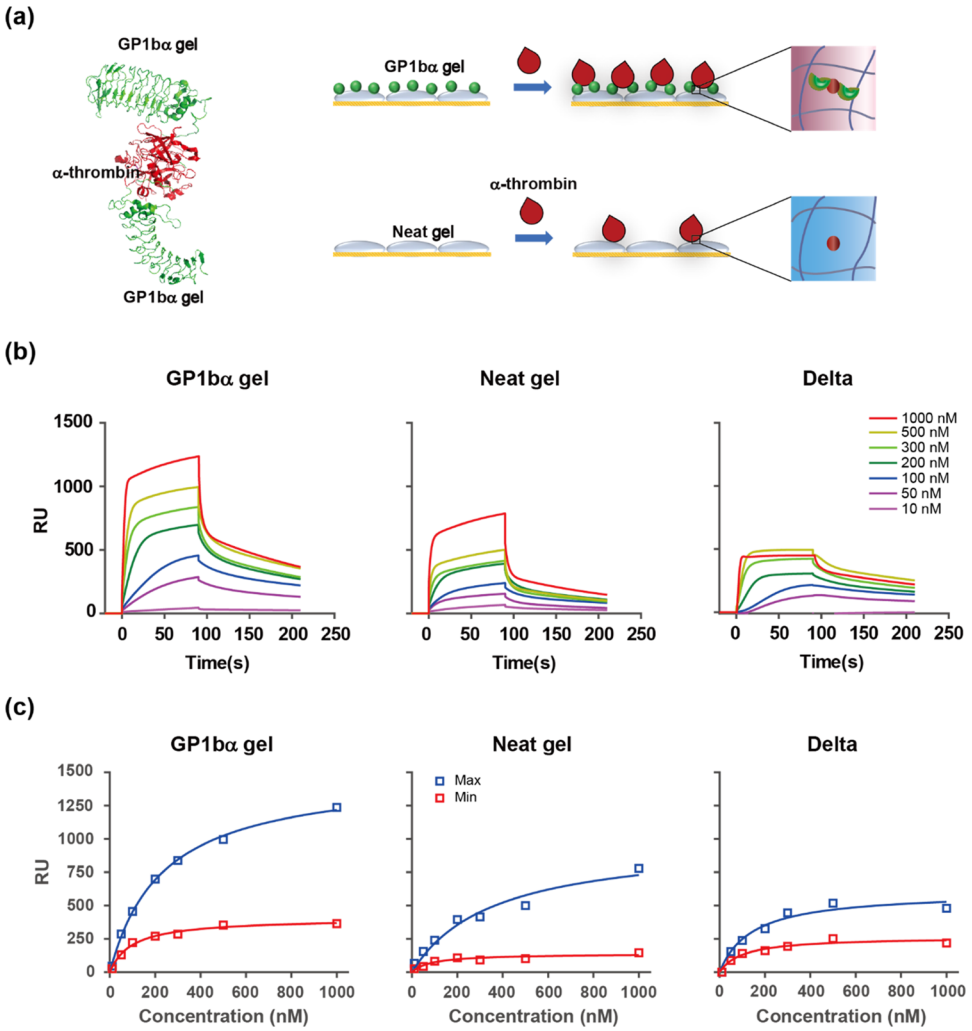

Figure 1. SRP analysis of GPIbα-functionalized nanogels in response to α-thrombin binding reveals that MPB provides a path for α-thrombin detection. (a) (Left) Molecular structure of the α-thrombin−GPIbα complex reconstructed by X-ray crystallography showing MPB. (Right) Schematic showing that the GPIbα-functionalized nanogel undergoes deswelling and changes in its RI in response to α-thrombin binding, whereas the neat nanogel does not. (b) RU curves of the GPIbα-functionalized nanogel (left), neat nanogel (middle), and the difference between the curves (right) in response to 10 nM (pink), 50 nM (purple), 100 nM (blue), 200 nM (green), 300 nM (light green), 500 nM (yellow), or 1000 nM (red) α-thrombin flow. (c) RU_{max} (blue square) and RU_{min} values (red square) of the GPIbα-functionalized nanogel (left), neat nanogel (middle), and the difference between these values (right). Fitting lines with the Langmuir model are also plotted for RU_{max} (blue line) and RU_{min} (red line).

dissociation time was 120 s. For the reference channel, a GPIbα solution without α-thrombin was injected. The sensorgram was recorded using the embedded imSPR-min software.

2.7. DLS Analysis. The hydrodynamic diameter of the nanogels was measured at a detection angle of 173° using a Zetasizer Pro (Malvern Instruments, Worcestershire, U.K.), equipped with a 633 nm He−Ne laser. Measurements were performed at 25 °C with deionized water as a dispersant in disposable polystyrene (PS) cuvettes.

2.8. ELISA Analysis. The GPIbα stock solution (250 μg/mL) was diluted with PBS buffer to various concentrations. Each GPIbα solution (50 μL) was added to a Ni-NTA plate (Qiagen, Venlo, Netherlands), followed by overnight incubation at 4 °C. The plate was rinsed three times with 200 μL of PBS and incubated with 100 μL of 1% bovine serum albumin for 30 min at room temperature (20−25 °C, RT). After the removal of the blocking buffer, the plate was filled with 50 μL of the α-thrombin solution at various concentrations, followed by incubation for 1 h at RT. Subsequently, the wells were rinsed three times with the washing buffer. For labeling of the captured α-thrombin, 50 μL of biotinylated primary antibody (Novus Biologicals, Centennial, CO) was added to the wells, followed by incubation for 1 h and five rinses. The wells were then treated with peroxidase-conjugated streptavidin (Novus Biologicals), followed by a 30 min incubation and five rinses. To generate the absorption spectra, 50 μL of the chromogen substrate was added to each well, followed by incubation for 10 min. The absorbance was measured at 570 nm at this point, and the absorbance at 450 nm was measured after the addition of 50 μL of the stop solution using a UV−vis microplate spectrophotometer (SpectraMax iD3, Molecular Devices, LLC, San Jose, CA).

2.9. Latex Agglutination (LA) Analysis. A total of 100 μL of PS beads (2.5% w/v, 0.1−0.2 μm; Spherotech, Inc., Lake Forest, IL) was centrifuged at 13,000 rpm for 20 min at 20 °C, resuspended in 200 μL of MES buffer (pH 5.5, 0.1 M), and centrifuged at 13,000 rpm for 20 min at 20 °C. Subsequently, 25 μL of EDC (100 mg/mL) and 25 μL of 50 mM NTA were added to the PS solution and incubated for 1 h at RT. The

https://doi.org/10.1021/acsomega.4c00010
ACS Omega 2024, 9, 13418−13426

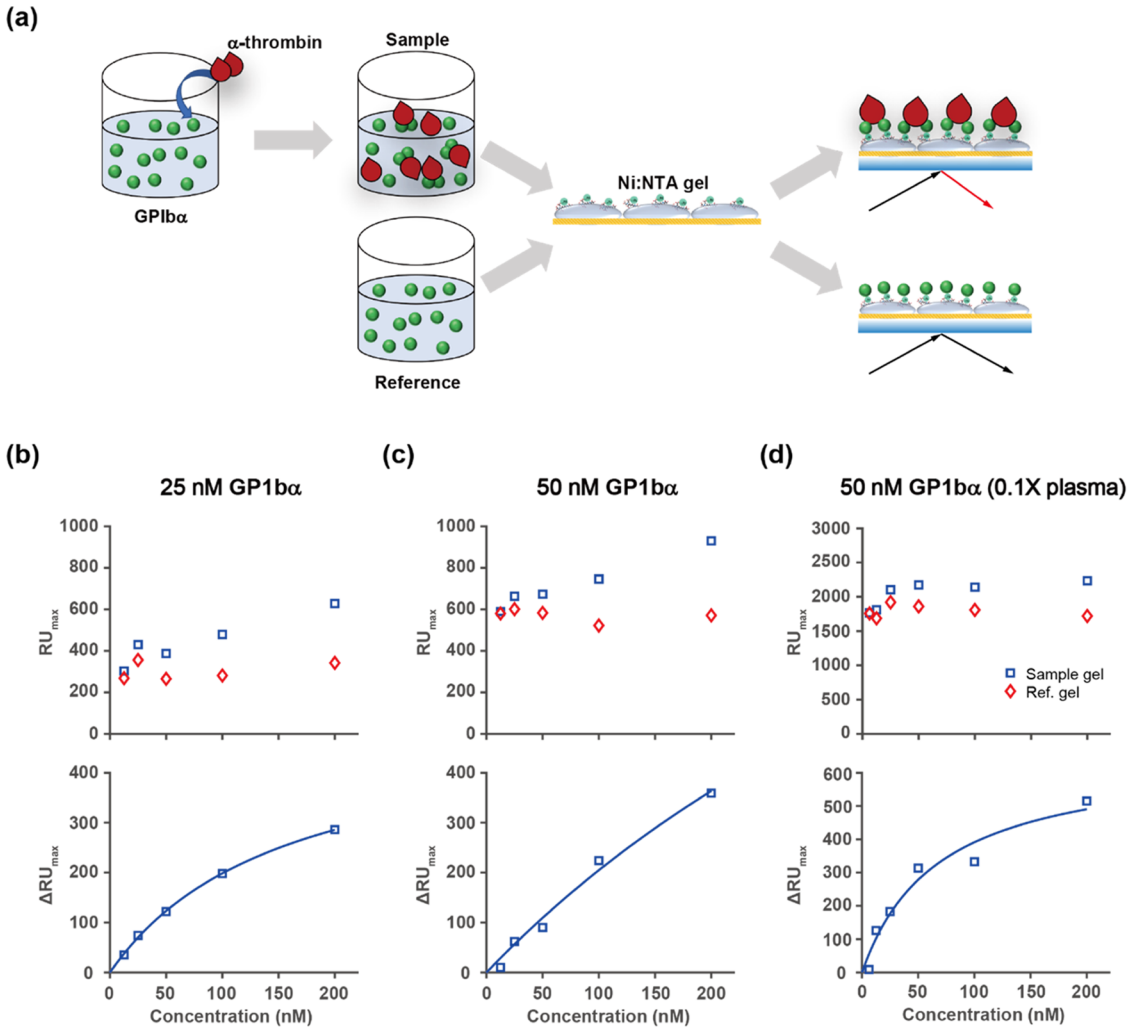

Figure 2. SPR analysis of Ni^{2+}:NTA-functionalized nanogels in response to α-thrombin−GPIbα complex binding shows that MPB can be strategically used for the sensitive detection of α-thrombin in clinical samples. (a) Schematic showing that Ni^{2+}:NTA-functionalized nanogel undergoes changes in its RI in response to α-thrombin−GPIbα complex binding. (b) (Top) RU_{max} values from sample (blue squares) and reference (red squares) channels for 25 nM GPIbα preincubated with buffered samples plotted as a function of α-thrombin concentration. (Bottom) The delta RU_{max} values (blue squares) plotted as a function of α-thrombin concentration together with the Langmuir model fitting line (blue line). (c) (Top) RU_{max} values from sample (blue squares) and reference (red squares) channels for 25 nM GPIbα preincubated with buffered samples plotted as a function of α-thrombin concentration. (Bottom) The delta RU_{max} values for 50 nM GPIbα (blue squares) plotted as a function of α-thrombin concentration together with the Langmuir model fitting line (blue line). (d) (Top) RU_{max} values from sample (blue squares) and reference (red squares) channels for 50 nM GPIbα preincubated with plasma samples plotted as a function of α-thrombin concentration. (Bottom) The delta RU_{max} values (blue squares) plotted as a function of α-thrombin concentration together with the Langmuir model fitting line (blue line).

reaction mixture was purified by removing unreacted EDC, NHS, and NTA by centrifugation, resuspended five times in 500 μL of 0.001% triton-X 100 solution, and then dissolved in 350 μL of 0.001% triton-X 100 and 0.05% sodium azide solution. A $NiCl_2$ solution was added to obtain a final concentration of 0.5 mM and to form Ni-NTA-functionalized PS beads. The functionalized nanogels were stored at 4 °C. Ni-NTA PS beads were mixed with polyhistidine-tagged (6× His) GPIbα (final concentration: 100 nM) to prepare GPIbα-coated beads. For the α-thrombin measurement, 10 μL of GPIbα PS beads was mixed with 10 μL of a sample solution at various concentrations. The mixture was then analyzed by using DLS analysis or a NanoDrop Spectrometer (Thermo Fisher Scientific, Waltham, MA).

3. RESULTS AND DISCUSSION

3.1. SPR Analysis. GPIbα dimerization via α-thrombin (Figure 1a) is not only a pivotal step in the clotting cascade but also useful for the highly sensitive and selective detection of α-thrombin. To prepare the sensing platform for bioresponsive nanogel-based SPR (nSPR) analysis, nanogels were functionalized with the extracellular domain of GPIbα proteins via *ex situ* EDC/NHS coupling and injected into the measurement channel, whereas neat nanogels were introduced to the reference channel. In response to α-thrombin injection, the GPIbα-functionalized nanogel was designed to undergo changes in RI via MPB (Figure 1a),[26] causing signatures in the nSPR signal. As the α-thrombin concentration increased, the association features in the sensorgram became sharper, followed by a sharper decay (Figure 1b). Similar features with reduced peak heights were also observed in the sensorgrams of the reference channel, which were produced by nonspecific

https://doi.org/10.1021/acsomega.4c00010
ACS Omega 2024, 9, 13418−13426

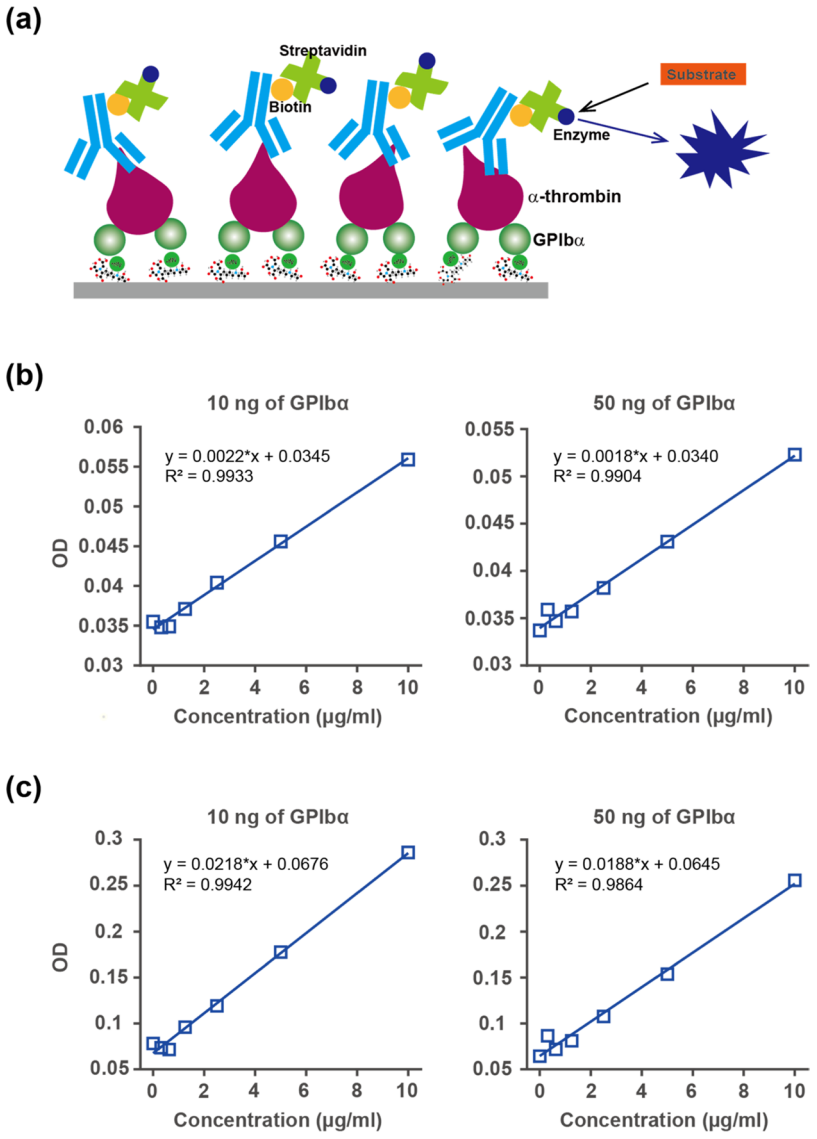

Figure 3. ELISA analysis with GPIbα as the capture handle allows the characterization of the α-thrombin standard solution. (a) Schematic showing that the GPIbα-passivated microplate captured α-thrombin and underwent antibody binding and enzyme−substrate reactions to generate the specific signal. (b) OD values (blue rectangles) at 570 nm plotted as a function of α-thrombin concentration for 10 ng (left) and 50 ng (right) of GPIbα passivation; linear fits (blue lines). (c) OD values (blue rectangles) at 450 nm plotted as a function of α-thrombin concentration for 10 ng (left) and 50 ng (right) of GPIbα passivation; linear fits (blue lines).

interactions. The delta sensorgrams generated by subtracting nonspecific signals from the corresponding sample signals represent the specific binding of α-thrombin to GPIbα on nanogels via MPB events (Figure 1b).

To investigate whether the nSPR analysis enables quantification of α-thrombin, the maximum and minimum values of the sensorgrams were plotted as a function of the α-thrombin concentration. The resonance unit maximum (RU_{max}) and minimum (RU_{min}) values from the GPIbα gel sensorgrams (Figure 1c) increased with α-thrombin concentration but became less inclined at higher concentrations. After subtraction of these values in the neat gel sensorgrams, the RU_{max} and RU_{min} curves from the delta sensorgrams were plotted, exhibiting a decent correlation with α-thrombin concentrations, and those values were detectable except at 10 nM. Both RU_{max} and RU_{min} curves in the delta plot have a plateau region from 500 nM to 1 μM, implying a reduced signal-to-noise ratio (SNR) at this high concentration regime. To check whether this is the case, ratios of signals (RU values in the GPIbα gel) to noises (RU values in the neat gel) were plotted in Figure S4, showing the lowered SNR at 1 μM compared to others.

The features of the RU curves reflect the kinetics of MPB between the receptor and the ligand. The RU_{max} and RU_{min} curves were fitted to the Langmuir model to obtain a quantitative understanding of the origin of these features. The fitting parameters shown in Table S1 are equilibrium constants, which are inversely correlated to the transition points in the RU curves. The value of each RU_{max} curve was less than that of the corresponding RU_{min} curve, indicating that RU_{max} has a wider dynamic range than RU_{min}. Because both RU values exhibit similar fluctuation levels with respect to fits, it is reasonable to choose RU_{max} as the criterion for the quantification of α-thrombin in nSPR analysis.

The nSPR protocol described above is beneficial for gaining insight into the precise kinetics of the MPB reactions.

https://doi.org/10.1021/acsomega.4c00010
ACS Omega 2024, 9, 13418−13426

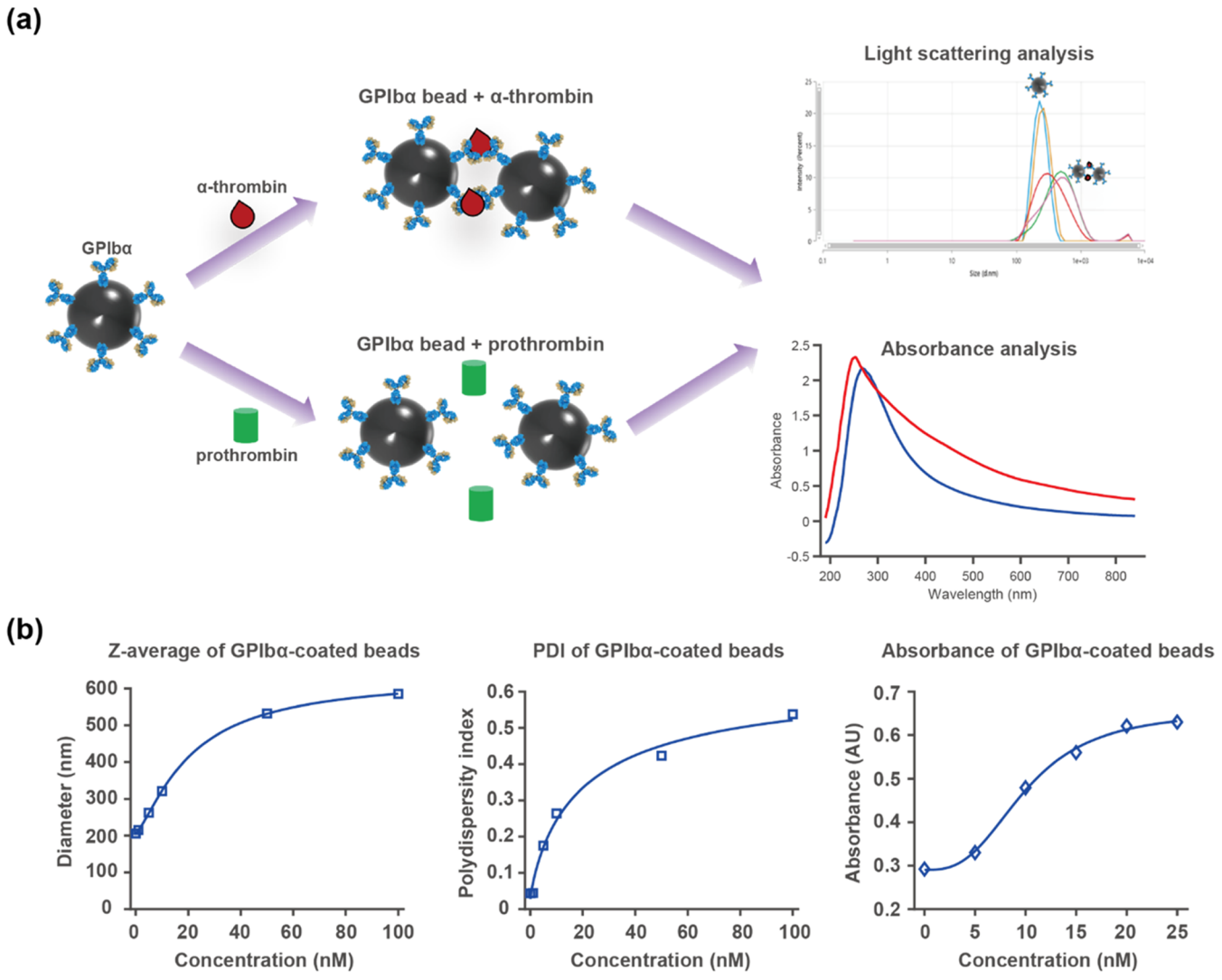

Figure 4. GPIbα-functionalized latex bead agglutination analyses demonstrated the detection of α-thrombin with hospital instruments. (a) Schematic showing that the GPIbα-coated PS beads become multimerized in response to α-thrombin binding. Multimerized beads lead to greater peak values in DLS analysis and a blue shift in absorbance analysis. (b) (Left) *Z*-average values (blue squares) of buffer samples plotted as a function of α-thrombin concentration. (Middle) PDI values (blue squares) of buffer samples plotted as a function of α-thrombin concentration. (Right) Absorbance values (blue diamonds) of buffer samples plotted as a function of α-thrombin concentration. The Hill model fitting line (blue line) is plotted together with each data set.

However, the handling of patient samples requires different experimental procedures. To achieve higher sensitivity in the nSPR analysis, which is a prerequisite for α-thrombin detection in patient samples, another experimental protocol was tested. In this protocol, the nanogels were functionalized with Ni^{2+}-charged NTA via *ex situ* EDC/NHS coupling and loaded into both measurement and reference channels (Figure 2a). To measure α-thrombin, 6× His GPIbα was preincubated with either an α-thrombin solution or a PBS-buffered solution, and then each sample flowed into the corresponding channel. Herein, MPB-like complexes were formed and captured by Ni^{2+}-charged NTA nanogels only when α-thrombin was present, whereas intact 6× His GPIbα monovalently interacted with Ni-NTA (Figure 2a). This approach is advantageous for improving the capturing efficiency because soluble GPIbα has a higher cross section to interact with α-thrombin compared to that of nanogel-immobilized GPIbα.

To optimize the experimental conditions, SPR analysis with 25 or 50 nM GPIbα for complex production was performed for the detection and quantification of α-thrombin in the buffered solution. Herein, we focused only on the RU_{max} analysis because of its higher dynamic range. To get a sense of SNR in each experimental setting, the RU_{max} values of sample and reference channels were plotted for those two GPIbα concentrations, as depicted in Figure 2b,c. As shown clearly, paired RU_{max} values of those two channels seem to be correlated, and overall, signals at the reference channel for the 50 nM GPIbα setting are about two times higher than those for the 25 nM GPIbα setting probably due to monovalent binding of 6× His GPIbα to Ni-NTA on a gold chip. SNR values (defined by the ratio of the signal at the sample channel to that at the reference channel) were plotted in Figure S4, showing differences in these values between the two experimental settings. The delta RU_{max} values that are obtained by subtraction of the reference signal from the sample signal are also plotted for each GPIbα concentration (Figure 2b,c). At both 25 and 50 nM GPIbα, the delta RU_{max} curve tended to increase with the α-thrombin concentration. However, there

https://doi.org/10.1021/acsomega.4c00010
ACS Omega 2024, 9, 13418−13426

were some differences in the features of these curves. The lowest α-thrombin concentration (12.5 nM) led to a delta RU_{max} value at 25 nM higher than that at 50 nM. By contrast, the curve at 50 nM displayed a better linearity between the α-thrombin concentration and the delta RU_{max} value.

The distinct curve features dependent on the GPIbα concentration were further analyzed by using Langmuir model fitting to investigate the optimal preincubation conditions. The fitting of these RU_{max} curves resulted in equilibrium constant values of 0.0064 ± 0.0004 and 0.0015 ± 0.0011 nM^{-1} for 25 and 50 nM GPIbα samples, respectively. This indicates that the number of binding sites provided by incubation with 25 nM GPIbα could not cover hundreds of nanomolar α-thrombin concentrations, whereas 50 nM GPIbα was sufficient for that concentration range. This fact should be considered for the measurement of α-thrombin in plasma samples because it was previously known that the association reaction is faster in the plasma than in the buffer.[28]

Preincubation of undiluted plasma samples with a 50 nM GPIbα solution is expected to greatly accelerate the association reaction even at very low concentrations. Therefore, plasma was diluted 10 times, incubated with 6× His GP1bα for complex formation, and used for nSPR analysis. The RU_{max} values from sample and reference channels are plotted in Figure 2d, revealing higher noise floors compared to those in buffered samples (the SNR plot in Figure S4). The delta RU_{max} values shown in Figure 2d indicate that α-thrombin in the plasma was detectable except at the lowest concentration (6.25 nM). The delta RU_{max} curve exhibited linearity with a reasonable dynamic range, with a quantifiable α-thrombin concentration of up to 200 nM. Taken together, these results suggest that SPR analysis with our sensor platform is suitable for the detection and quantification of α-thrombin in clinical settings.

3.2. ELISA Analysis. The binding mode of GPIbα to α-thrombin has the potential to facilitate the detection of α-thrombin by immunochemistry analysis in outpatient settings. We tested GPIbα as a capture molecule in ELISA to ensure that the binding reaction was useful for this gold-standard technique (Figure 3a). Each microplate was incubated with 10 or 50 ng of GPIbα overnight and used to capture α-thrombin in a standard solution. Subsequently, α-thrombin was labeled via antibody binding, enzyme−substrate reaction, and light attenuation was measured at 570 nm. As shown in Figure 3b, regardless of the GPIbα concentration, the optical density (OD) of each sample correlated well with its α-thrombin concentration. Both graphs display linear relationships but with very high baselines. This indicated that 10 ng of GPIbα was sufficient to cover the microplate area and generate an optimal number of capture handles, whereas 50 ng of GPIbα seemed to be superfluous. However, the result also revealed that the 570 nm channel was not an optimal choice for the measurement in terms of the SNR.

To achieve signal enhancement in ELISA, another set of experiments was conducted with the stop solution of the enzyme−substrate reaction. Subsequently, the light attenuation of each sample was measured at 450 nm. As shown in Figure 3c, new graphs featured signal-to-background ratios higher than those of the corresponding ones shown in Figure 3b. Their slopes increased by approximately ten times; however, the baselines increased only approximately two times. Both 10 and 50 ng of GPIbα produced excellent linearity in the corresponding graph. In other words, we demonstrated that GPIbα, as a capturing molecule, instead of an antibody, was suitable for the detection and quantification of α-thrombin in ELISA analysis.

3.3. LA Assays. Although nSPR analysis using the nanogel sensing platform successfully achieved α-thrombin detection in plasma samples, simpler experimental procedures with hospital instruments are desirable for the clinical application of such detection methods. In this section, we describe LA-based methods developed as an alternative to ELISA for α-thrombin detection in an outpatient setting. As shown in Figure 4a, the dual binding of α-thrombin with the two GPIbα-coated beads can induce bead aggregation. This assay was used for α-thrombin detection in a buffer solution. The hydrodynamic diameter and polydispersity index (PDI) of the beads were measured for samples with α-thrombin concentrations ranging from 0 to 100 nM. The *Z*-average of the bead diameter increased from 200 nM and saturated above ∼60 nM (Figure 4b, left). The PDI of the GPIbα-coated beads exhibited an even larger incremental rate without being saturated until a concentration of 100 nM was reached (Figure 4b, middle). These samples were also analyzed based on changes in their optical absorbance; the value was ∼0.3 at zero concentration and increased to ∼0.67 at 30 nM (Figure 4b, right). Overall, these three curves were S-shaped with plateau regions close to zero.

As an easy-to-use tool for the detection of coagulation markers, LA assays should be competitive with ELISA in terms of rapidity, sensitivity, and dynamic range. Preparation and measurement times of these assays are generally much shorter than those of ELISA. To assess the detection performance, nonlinear model fitting was performed on the curves shown in Figure 4b. Instead of the Langmuir model, S-shaped curves were fitted to the Hill equation. The calculated half-occupancy concentrations were sequentially 20.97, 20.67, and 10.00 nM for those curves. This indicates that DLS and absorbance analysis can detect α-thrombin concentrations less than tens of nanomoles, which is comparable to that of ELISA analysis. These results suggest the potential use of GPIbα-coated beads in the clinical application of α-thrombin detection.

4. CONCLUSIONS

α-Thrombin, a key regulatory protein in the blood coagulation cascade, represents an important target for early thromboembolism diagnosis. In this study, we developed analytical modalities for α-thrombin detection based on its specific binding to the platelet protein GPIbα and tested different methods to investigate in-depth detection protocols via MPB and to demonstrate easy and timely detection of this candidate marker. Our nanogel platform, known for its proficiency in ligand detection such as IL-2 and SARS-COV-2 in SPR analysis,[28,30] was used by functionalizing it with GPIbα. The nSPR assay indicated that GPIbα was suitable for α-thrombin detection with not only high-fidelity binding but also wide dynamic ranges. The application of the Ni-NTA-functionalized nanogel and 6× His GP1bα for nSPR analysis enabled the quantification of α-thrombin in the plasma. In addition, the use of GPIbα for α-thrombin detection was validated by ELISA and LA assays. Notably, our LA-based methods with a short time frame (∼5 min) exhibited performance comparable to that of ELISA, suggesting that the MPB of GPIbα to α-thrombin will provide an avenue for the clinical application of α-thrombin detection methods. Importantly, our study will contribute to advancing patient care in the context of blood

https://doi.org/10.1021/acsomega.4c00010
ACS Omega 2024, 9, 13418−13426

coagulation disorders. Nonvitamin K antagonist oral anticoagulants (NOAC), a newly categorized class of oral anticoagulants that directly or indirectly antagonize α-thrombin, are currently prevalent in treating patients with atrial fibrillation and prevent thromboembolism.[31−33] However, their safe and efficacious use requires regular monitoring of blood coagulation potency with high precision. Current methods, such as PT/INR and aPTT, only provide limited information as they do not directly measure coagulation factors.[34] Therefore, our GPIbα-functionalized modality for α-thrombin will be an excellent tool for gauging the effectiveness of NOACs in that it enables the rapid and selective detection of this marker protein. Our findings suggest that GPIbα-based assays are robust candidates for the clinical measurement of α-thrombin, offering insights into coagulation status.

■ ASSOCIATED CONTENT

Supporting Information

The Supporting Information is available free of charge at https://pubs.acs.org/doi/10.1021/acsomega.4c00010.

Figures S1−S4 and Table S1: ^{1}H nuclear magnetic resonance (NMR) spectra, atomic force microscopy (AFM) images, volume phase transition (VPT) plot, count rate in DLS data vs size, SNR plots, and a table of fit parameters. (PDF)

■ AUTHOR INFORMATION

Corresponding Authors

Yongdoo Park − *Department of Biomedical Sciences, College of Medicine, Korea University, Seoul 02841, Republic of Korea;* orcid.org/0000-0003-3822-4651; Email: ydpark67@korea.ac.kr

Jongseong Kim − *R&D Center, Scholar Foxtrot Co. Ltd., Seoul 02796, Republic of Korea; Department of Biomedical Sciences, College of Medicine, Korea University, Seoul 02841, Republic of Korea;* orcid.org/0000-0001-9595-2765; Email: envokim72@korea.ac.kr

Authors

Doogie Oh − *R&D Center, Scholar Foxtrot Co. Ltd., Seoul 02796, Republic of Korea; Department of Biomedical Sciences, College of Medicine, Korea University, Seoul 02841, Republic of Korea*

Yun Jin Chae − *R&D Center, Scholar Foxtrot Co. Ltd., Seoul 02796, Republic of Korea*

Jie Ying Teoh − *Department of Chemical and Biological Engineering, Institute of Chemical Processes, Seoul National University, Seoul 08826, Republic of Korea*

Bora Yim − *R&D Center, Scholar Foxtrot Co. Ltd., Seoul 02796, Republic of Korea*

Dongwon Yoo − *Department of Chemical and Biological Engineering, Institute of Chemical Processes, Seoul National University, Seoul 08826, Republic of Korea; Center for Nanoparticle Research, Institute for Basic Science (IBS), Seoul 08826, Republic of Korea;* orcid.org/0000-0002-4547-6948

Complete contact information is available at: https://pubs.acs.org/10.1021/acsomega.4c00010

Author Contributions

The manuscript was written through contributions of all authors. All authors have given approval to the final version of the manuscript.

Notes

The authors declare no competing financial interest.

■ ACKNOWLEDGMENTS

J.K. acknowledges the financial support from the National Research Foundation of Korea (NRF-2022R1I1A1A01064249). Y.P. acknowledges the financial support from the National Research Foundation of Korea (NRF-2019M3D1A1078940).

■ REFERENCES

(1) Crawley, J. T.; Zanardelli, S.; Chion, C. K.; Lane, D. A. The central role of thrombin in hemostasis. *J. Thromb. Haemostasis* **2007**, *5* (Suppl 1), 95−101.

(2) Tripodi, A.; Legnani, C.; Chantarangkul, V.; Cosmi, B.; Palareti, G.; Mannucci, P. M. High thrombin generation measured in the presence of thrombomodulin is associated with an increased risk of recurrent venous thromboembolism. *J. Thromb. Haemostasis* **2008**, *6* (8), 1327−1333.

(3) Danese, E.; Montagnana, M.; Cervellin, G.; Lippi, G. Hypercoagulability, D-dimer and atrial fibrillation: an overview of biological and clinical evidence. *Ann. Med.* **2014**, *46* (6), 364−371.

(4) Connolly, S. J.; Ezekowitz, M. D.; Yusuf, S.; Eikelboom, J.; Oldgren, J.; Parekh, A.; Pogue, J.; Reilly, P. A.; Themeles, E.; Varrone, J.; et al. Dabigatran versus Warfarin in Patients with Atrial Fibrillation. *N. Engl. J. Med.* **2009**, *361* (12), 1139−1151.

(5) Patel, M. R.; Mahaffey, K. W.; Garg, J.; Pan, G.; Singer, D. E.; Hacke, W.; Breithardt, G.; Halperin, J. L.; Hankey, G. J.; Piccini, J. P.; et al. Rivaroxaban versus Warfarin in Nonvalvular Atrial Fibrillation. *N. Engl. J. Med.* **2011**, *365* (10), 883−891.

(6) Granger, C. B.; Alexander, J. H.; McMurray, J. J. V.; Lopes, R. D.; Hylek, E. M.; Hanna, M.; Al-Khalidi, H. R.; Ansell, J.; Atar, D.; Avezum, A.; et al. Apixaban versus Warfarin in Patients with Atrial Fibrillation. *N. Engl. J. Med.* **2011**, *365* (11), 981−992.

(7) van Veen, J. J.; Smith, J.; Kitchen, S.; Makris, M. Normal prothrombin time in the presence of therapeutic levels of rivaroxaban. *Br. J. Hamaetol.* **2013**, *160* (6), 859−861.

(8) Wadsworth, D.; Sullivan, E.; Jacky, T.; Sprague, T.; Feinman, H.; Kim, J. A review of indications and comorbidities in which warfarin may be the preferred oral anticoagulant. *J. Clin. Pharm. Ther.* **2021**, *46* (3), 560−570.

(9) Chen, B.; Wang, Y.; Shen, S.; Zhong, W.; Lu, H.; Pan, Y. Lattice Defects and Electronic Modulation of Flower-Like Zn3In2S6 Promote Photocatalytic Degradation of Multiple Antibiotics. *Small Methods* **2024**, No. 2301598.

(10) Ruggeri, Z. M. The role of von Willebrand factor in thrombus formation. *Thromb. Res.* **2007**, *120* (Suppl 1), S5−S9.

(11) Springer, T. A. von Willebrand factor, Jedi knight of the bloodstream. *Blood* **2014**, *124* (9), 1412−1425.

(12) De Luca, M.; Facey, D. A.; Favaloro, E. J.; Hertzberg, M. S.; Whisstock, J. C.; McNally, T.; Andrews, R. K.; Berndt, M. C. Structure and function of the von Willebrand factor A1 domain: analysis with monoclonal antibodies reveals distinct binding sites involved in recognition of the platelet membrane glycoprotein Ib-IX-V complex and ristocetin-dependent activation. *Blood* **2000**, *95* (1), 164−172.

(13) Nowak, A. A.; Canis, K.; Riddell, A.; Laffan, M. A.; McKinnon, T. A. O-linked glycosylation of von Willebrand factor modulates the interaction with platelet receptor glycoprotein Ib under static and shear stress conditions. *Blood* **2012**, *120* (1), 214−222.

(14) Chen, J.; Lopez, J. A. Interactions of platelets with subendothelium and endothelium. *Microcirculation* **2005**, *12* (3), 235−246.

(15) Zhang, X.; Halvorsen, K.; Zhang, C. Z.; Wong, W. P.; Springer, T. A. Mechanoenzymatic cleavage of the ultralarge vascular protein von Willebrand factor. *Science* **2009**, *324* (5932), 1330−1334.
(16) Mazzucato, M.; De Marco, L.; Masotti, A.; Pradella, P.; Bahou, W. F.; Ruggeri, Z. M. Characterization of the Initial α-Thrombin Interaction with Glycoprotein Ibα in Relation to Platelet Activation. *J. Biol. Chem.* **1998**, *273* (4), 1880−1887.
(17) Dumas, J. J.; Kumar, R.; Seehra, J.; Somers, W. S.; Mosyak, L. Crystal Structure of the GpIbalpha-Thrombin Complex Essential for Platelet Aggregation. *Science* **2003**, *301* (5630), 222−226.
(18) Celikel, R.; McClintock, R. A.; Roberts, J. R.; Mendolicchio, G. L.; Ware, J.; Varughese, K. I.; Ruggeri, Z. M. Modulation of alpha-thrombin function by distinct interactions with platelet glycoprotein Ibalpha. *Science* **2003**, *301* (5630), 218−221.
(19) Zarpellon, A.; Celikel, R.; Roberts, J. R.; McClintock, R. A.; Mendolicchio, G. L.; Moore, K. L.; Jing, H.; Varughese, K. I.; Ruggeri, Z. M. Binding of alpha-thrombin to surface-anchored platelet glycoprotein Ib(alpha) sulfotyrosines through a two-site mechanism involving exosite I. *Proc. Natl. Acad. Sci. U.S.A.* **2011**, *108* (21), 8628−8633.
(20) Estevez, B.; Kim, K.; Delaney, M. K.; Stojanovic-Terpo, A.; Shen, B.; Ruan, C.; Cho, J.; Ruggeri, Z. M.; Du, X. Signaling-mediated cooperativity between glycoprotein Ib-IX and protease-activated receptors in thrombin-induced platelet activation. *Blood* **2016**, *127* (5), 626−636.
(21) Mehta, A. Y.; Thakkar, J. N.; Mohammed, B. M.; Martin, E. J.; Brophy, D. F.; Kishimoto, T.; Desai, U. R. Targeting the GPIbalpha binding site of thrombin to simultaneously induce dual anticoagulant and antiplatelet effects. *J. Med. Chem.* **2014**, *57* (7), 3030−3039.
(22) Beck, S.; Oftering, P.; Li, R.; Hemmen, K.; Nagy, M.; Wang, Y.; Zarpellon, A.; Schuhmann, M. K.; Stoll, G.; Ruggeri, Z. M.; et al. Platelet glycoprotein V spatio-temporally controls fibrin formation. *Nat. Cardiovasc. Res.* **2023**, *2* (4), 368−382.
(23) Versteeg, H. H.; Heemskerk, J. W.; Levi, M.; Reitsma, P. H. New fundamentals in hemostasis. *Physiol. Rev.* **2013**, *93* (1), 327−358.
(24) Lane, D. A.; Philippou, H.; Huntington, J. A. Directing thrombin. *Blood* **2005**, *106* (8), 2605−2612.
(25) Dong, J.-F.; Berndt, M. C.; Schade, A.; McIntire, L. V.; Andrews, R. K.; López, J. A. Ristocetin-dependent, but not botrocetin-dependent, binding of von Willebrand factor to the platelet glycoprotein Ib-IX-V complex correlates with shear-dependent interactions. *Blood* **2001**, *97* (1), 162−168.
(26) Kim, J.; Park, Y.; Brown, A. C.; Lyon, L. A. Direct observation of ligand-induced receptor dimerization with a bioresponsive hydrogel. *RSC Adv.* **2014**, *4* (110), 65173−65175.
(27) Yang, H. M.; Teoh, J. Y.; Yim, G. H.; Park, Y.; Kim, Y. G.; Kim, J.; Yoo, D. Label-Free Analysis of Multivalent Protein Binding Using Bioresponsive Nanogels and Surface Plasmon Resonance (SPR). *ACS Appl. Mater. Interfaces* **2020**, *12* (5), 5413−5419.
(28) Yang, H. M.; Yim, B.; Lee, B. H.; Park, Y.; Kim, Y. G.; Kim, J.; Yoo, D. New Tool for Rapid and Accurate Detection of Interleukin-2 and Soluble Interleukin-2 Receptor alpha in Cancer Diagnosis Using a Bioresponsive Microgel and Multivalent Protein Binding. *ACS Appl. Mater. Interfaces* **2021**, *13* (29), 33782−33789.
(29) Teoh, J. Y.; Jeon, S.; Yim, B.; Yang, H. M.; Hwang, Y.; Kim, J.; Lee, S. K.; Park, E.; Kong, T. Y.; Kim, S. Y.; et al. Tuning Surface Plasmon Resonance Responses through Size and Crosslinking Control of Multivalent Protein Binding-Capable Nanoscale Hydrogels. *ACS Biomater. Sci. Eng.* **2022**, *8* (7), 2878−2889.
(30) Lee, S. K.; Yim, B.; Park, J.; Kim, N. G.; Kim, B. S.; Park, Y.; Yoon, Y. K.; Kim, J. Method for the Rapid Detection of SARS-CoV-2-Neutralizing Antibodies Using a Nanogel-Based Surface Plasmon Resonance Biosensor. *ACS Appl. Polym. Mater.* **2023**, *5* (3), 2195−2202.
(31) Hicks, T.; Stewart, F.; Eisinga, A. NOACs versus warfarin for stroke prevention in patients with AF: a systematic review and meta-analysis. *Open Heart* **2016**, *3* (1), No. e000279.
(32) Hanley, C. M.; Kowey, P. R. Are the novel anticoagulants better than warfarin for patients with atrial fibrillation? *J. Thorac. Dis.* **2015**, *7* (2), 165−171, DOI: 10.3978/j.issn.2072-1439.2015.01.23.
(33) Carnicelli, A. P.; Hong, H.; Connolly, S. J.; Eikelboom, J.; Giugliano, R. P.; Morrow, D. A.; Patel, M. R.; Wallentin, L.; Alexander, J. H.; Cecilia Bahit, M.; et al. Direct Oral Anticoagulants Versus Warfarin in Patients With Atrial Fibrillation: Patient-Level Network Meta-Analyses of Randomized Clinical Trials With Interaction Testing by Age and Sex. *Circulation* **2022**, *145* (4), 242−255.
(34) Patel, J. P.; Byrne, R. A.; Patel, R. K.; Arya, R. Progress in the monitoring of direct oral anticoagulant therapy. *Br. J. Hamaetol.* **2019**, *184* (6), 912−924.

https://doi.org/10.1021/acsomega.4c00010
ACS Omega 2024, 9, 13418−13426